GAS-BEARING DESIGN
SUPPORTED BY ARTIFICIAL INTELLIGENCE

One of the most discussed issues at the Gas Bearing Workshop 2023 was how artificial intelligence (AI) is being applied to reduce the computational efforts for designing gas bearings. Several presenters shared their experiences with this new way of working. Presentations of other developments and new guidelines in the field of foil bearings, herringbone-grooved bearings, coatings for foil bearings, and porous bearings showed that these also stretch the boundaries of potential gas-bearing applications, of which several examples were highlighted.

JOS GUNSING

Programme

- Opening remarks
  Wolfram Runge (chairman), Berliner Hochschule für Technik, Germany
- Design for Stability: Insights in Porous Bearing Design
  Joep Nijssen, ASML, Veldhoven, the Netherlands
- Research on Gas Foil Bearings at TU Berlin
  Marian Sarazzin, Technische Universität Berlin, Germany
- Analysis of a Spindle supported by Aerostatic Bearings with External Damping Elements
  Federico Colombo, Politecnico di Torino, DIMEAS, Department of Mechanical and Aerospace Engineering, Turin, Italy
- Development of a Large Tomography Stage
  Koen Peeters, LAB Motion Systems, Leuven, Belgium
- Air Bearings for Environmental Credits, Turbo Application Examples
  Drew Devitt, New Way Air Bearings, Aston, USA
- Coating Wear Testing of Air Foil Bearings to Validate Fuel Cell System Applications
  Duc Ha, Omega Dot, Worcester Park, UK
- Modelling Approaches for the Design of Gas-Bearing Supported Rotors
  Jürg Schiffmann, EPFL, Lausanne, Switzerland
- Experimental Validation of Numerical Models for Rotordynamic Systems supported by Aerodynamic Bearings
  Elia Iseli, Fischer AG Präzisionsspindeln, Herzogenbuchsee, Switzerland

WWW.GAS-BEARING-WORKSHOP.COM

AUTHOR'S NOTE

Jos Gunsing is the founder/owner of MaromeTech, a technology & innovation support provider based in Nijmegen (NL), and a DSPE board member.

jos.gunsing@marometech.nl

Introduction

The Gas Bearing Workshop 2023, the fifth since the inaugural event in 2015, was organised by DSPE, VDE GMM and the *Bond voor Materialenkennis*. Luckily, this year the workshop was not delayed by Covid-19 and could be held as planned on 27 March, once again in Düsseldorf, Germany. The chair was split between organising committee members Wolfram Runge, Ron van Ostaijen, Farid Al-Bender and Jos Gunsing, with Wolfram Runge presenting the opening remarks and the wrap up.

Roughly, the focus items of the presenters were applied research, design including guidelines/methods, design of foil bearings, and special applications for high-speed compressor rotors and ultra-low-speed, highly accurate motion.
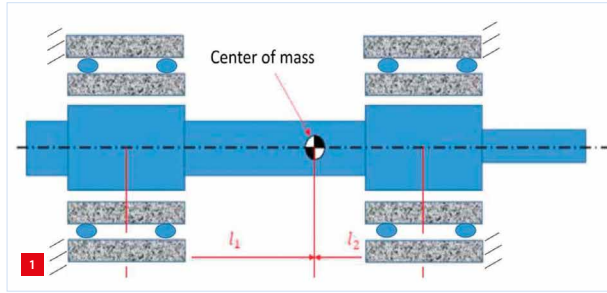
Schematic shaft and bearing layout with added spring/damping elements (O-rings) for each bearing.
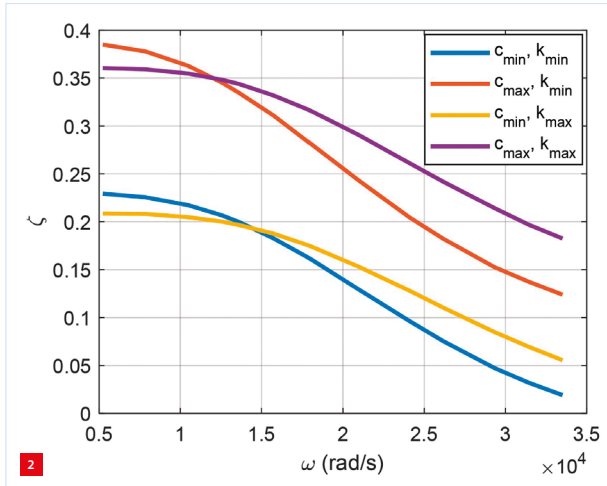
Damping ratio (linked to real and imaginary eigenvalues) versus speed for several combinations of stiffness (c) and damping (k). A damping ratio below zero indicates instability.

Joep Nijssen from ASML had permission to share results of his work only during the workshop itself, so his presentation will not be covered here.

Research & Design: damping elements

Federico Colombo (Politecnico Torino) presented work on the influence of additional damping elements on dynamic rotor stability. He set up models for a simple shaft layout (Figure 1) with and without extra O-ring-shaped spring/damping elements.

He found that the stability threshold could be improved dramatically by adding well-dimensioned spring/damping elements. Work was also carried out to investigate whether reducing the number of degrees of freedom to four would harm the prediction accuracy of instability thresholds. The simulation results can be seen in the graph of Figure 2

This graph presents the damping ratio (linked to real and imaginary eigenvalues) versus the rotational speed: if the damping ratio is below zero, instability will occur. The different colours represent the modes that are the most stability-sensitive for different stiffness/damping factor combinations. For the most sensitive mode shown here, the stability speed improved to approximately 320k rpm

with spring/damping O-rings applied, as compared to the situation without O-rings/fixed bushings (not in this graph; approximately 130k rpm).

In a separate study, the different O-ring materials were characterised in experiments. In the next research stage, extensive laboratory testing is planned to validate the model calculations/predictions. Tests are also planned at higher temperatures to determine whether the stiffness and damping characteristics will change.

Research & Design: foil bearings

Gas-foil bearings are of increasing interest for high-speed compressor applications in fuel cells. Here, gas (H_2, O_2/air mixture) has to be fed into the fuel cell with a certain pressure. Gas-foil bearings combine potentially low cost with low friction, long lifetime and smooth running at high speeds, as well as oil-free operation. Especially when it comes to automotive applications, the number of start-stop cycles is very high; more than 200k/250k problem-free start-stop cycles have to be realised.

This specific application gives also rise to several interesting research & design/development projects due to the specific automotive requirements.

Gas-foil bearing coatings
Duc Ha (Omega Dot) carried out intensive test work with respect to shaft or disc runner coatings counterface to the surface top foil (generally coated with Teflon) for gas-foil bearings, both for radial and axial bearings (Figure 3). Top-foil-coating wear was found to be the dominant bearing failure mechanism.

Several special test-rigs were designed and built in order to conduct a lot of high-cycle, start-stop test runs. Many materials were tested, such as TiN, WS_2, CrN, hard Cr, graphite/DLC, MoS_2 (also similar coating materials), with the uncoated counterface material as reference (bearing shaft or runner disc made of hardened steel, Teflon-coated top foil of foil bearing).

Naturally, the ideal material with respect to hardness level and low friction was not found (Figure 4), but CrN came close, the more so because it can be applied at a relatively low cost. In extended lifetime tests up to 250k cycles, CrN appeared to be performing very well, where both the bearing top foil and the uncoated counterface material already showed failures at 10k cycles or earlier.
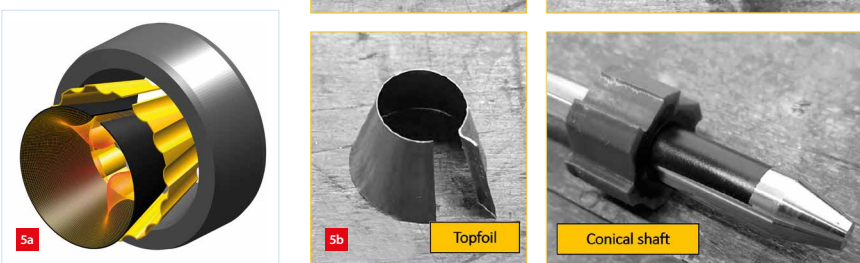
Conical gas-foil bearings
Marian Sarazzin (TU Berlin) presented an overview of the TU's work on foil bearings. Among other things, he presented work on the identification of damping and

Gas-foil bearings.
(a) Radial (journal).
(b) Axial (thrust).

Hardness versus friction coefficient for several counterface (shaft or disc runner) materials in contact with Teflon-coated top foils.

Conical gas-foil bearing.
(a) Overview.
(b) Components.

stiffness of structures and bearings, and tilting parameters plus their influence on the rotor stability of bearings. This was mainly experimental work as part of a funded research programme. Particularly interesting was his work on conical gas-foil bearings (Figure 5), which are able to support radial and axial loads, potentially saving space and cost. Of course, alignment and variation in preload due to manufacturing

tolerances including assembly/adjustment and thermal expansion during operation are important.

In Figure 6, the static behaviour/pressure distribution is simulated; the load-carrying capacity can be calculated/predicted in this way. The figure also shows the 3D dynamic behaviour/swirl of the rotor.

A new area that Sarazzin is moving into is research on gas-polymer bearings, both numerical and experimental, where a polymer layer will be applied in between the housing and the metal or PTFE (polytetrafluoroethylene) top foil (20-100 μm).

Special applications
Externally pressurised porous bearings for high-speed equipment
Drew Devitt (New Way Air Bearings) presented several applications of externally pressurised porous air bearings. He started with porous bearings for high-speed applications such as turbines and compressors. He described the case where externally pressurised porous bearings were replacing hydrodynamic oil bearings. Benefits include much lower frictional losses (Figure 7). His research was also focused on dynamic behaviour. It appeared in the analysis of the test results that the higher critical modes were more heavily damped.

Figure 8 shows the test-rig set-up with a double set of radial bearings (the second set not visible); in between the bearings, an eccentric balance mass was applied in order to introduce an imbalance load on the bearings. The test-rig on the right represents a typical turbine/compressor layout. The so-called Dresser-Rand rotor has been the subject of several research studies with respect to bearings and rotor stability.

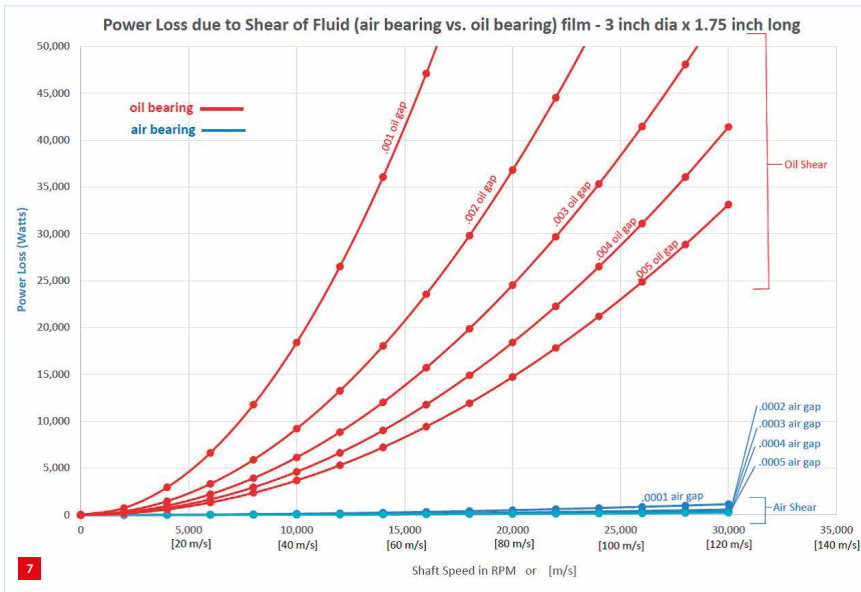*Externally pressurised porous bearing as seal*
Another example of the application of an externally pressurised porous bearing was a system that combined a seal and a thrust bearing. This combination offers relatively low friction and the opportunity to make a reliable division between process and other gasses in compressors/pumps. Figure 9 shows a schematic view and a cross-sectional design view of a real layout. By combining the bearing and the sealing function, a much less complicated design can be achieved, in this case with increased functionality, reliability and maintainability.

Ultra-low-speed application
Koen Peeters (LAB Motion Systems) described the motion system for an X-ray imaging machine (Figure 10) that will be applied for animal body parts, fossils, etc. It features high-precision motion of large samples up to 300 kg in five axes; overall resolution 0.2 μm, angular error max. 5 μrad and a sphere of confusion of 500 nm.
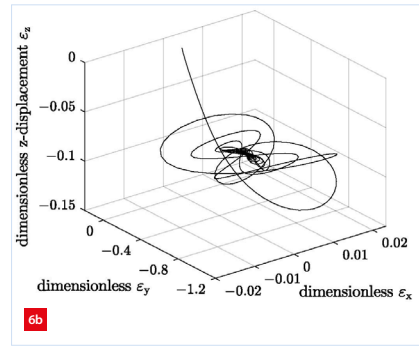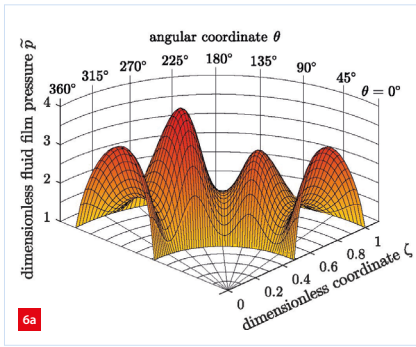
Simulation of a conical gas-foil bearing.
(a) Pressure distribution.
(b) Dynamic/swirl behaviour.

Typical differences in oil- versus gas-bearing friction losses.
Horizontal scale: shaft speed 0-35,000 rpm [0-140 m/s].
Vertical scale: power loss 0-50,000 W.
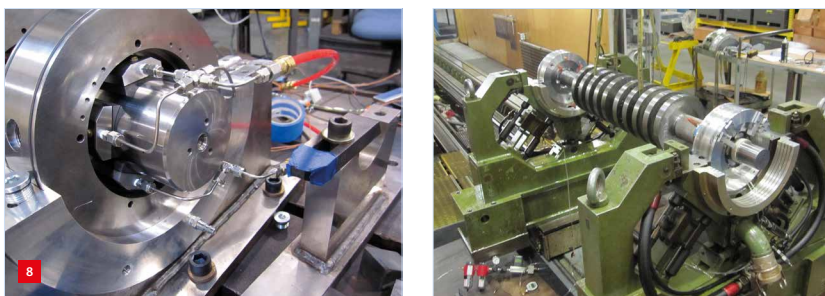
On the left, the test-rig for externally pressurised porous bearings (journal bearings). The bearing set-up was later transferred to the Dresser-Rand rotor on the right (test rotor for dynamic research, with a mass of 300 kg representing a typical turbine shaft).
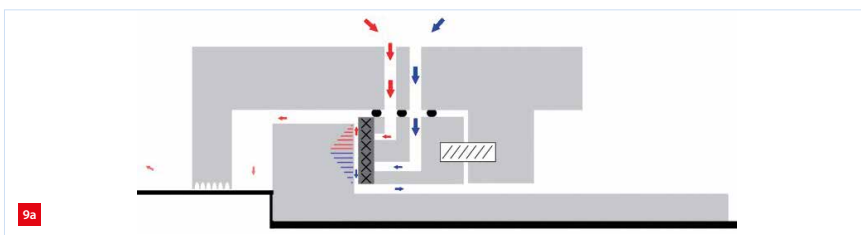
Thrust bearing acting as a seal; the externally pressurised porous bearing acts also as a balance piston.
(a) Schematic.   *(b)*   Design.

Several types of high-precision guideways were applied for vertical and horizontal motion stages, with the guideways mounted onto granite beams, including vertical motion and tilt correction driven by ball screws. The rotary stage on top was equipped with axial and radial air bearings. The metrology system was combined with an error-compensation system such that after calibration the high accuracies/resolution can be obtained. Figure 11 shows the typical repetitive radial run-out of the rotary table that can be compensated for.

An interesting part of Peeters' presentation was dedicated to "the reduction of vibration modes both in simulation and measurement". Thus, the simulation and optimisation time for this large, complex construction could be reduced to reasonable proportions.

AI-assisted modelling and validation

Robustness optimisation
Jürg Schiffmann (EPFL) focused on designing robust herringbone-grooved journal bearings. Domestic-scale heat-pump compressors (Figure 12) can be one order of magnitude more compact than piston-type compressors. Turbocompressors achieve a higher efficiency than positive-displacement machines, particularly in off-design conditions.

Further, using gas-lubricated bearings allows for the implementation of a fully oil-free solution, which is highly beneficial in heat pumps. Two types of gas bearings are applicable here. Herringbone-grooved journal bearings have high stability thresholds but require tight clearances. On the other hand, foil bearings with their compliant surface are tolerant to misalignment and thermal gradients. However, the interaction between fluid film and compliant structure (adding also damping) is complex and not well understood. Schiffmann's study focused on obtaining robust herringbone-grooved journal bearing designs with a manageable design effort in terms of simulation time and cost.

The current approach for designing complex, multi-disciplinary systems with competing design objectives is very often focused on the isolated design and optimisation of individual components. Hence, the overall optimum system performance is out of reach (Figure 13).
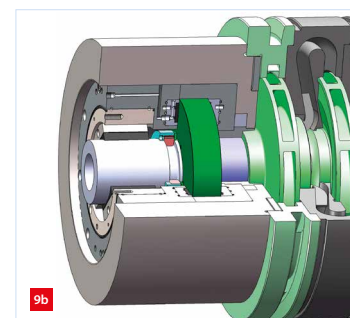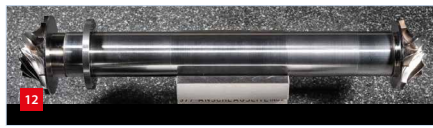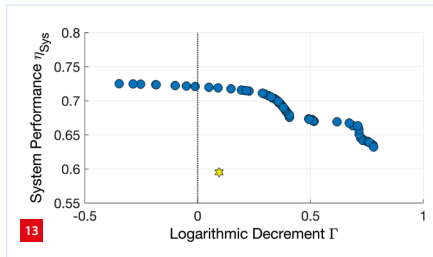
Support structure and rotary table with axial and radial air bearings for an X-ray imaging machine.
(a) Overview.
(b) Close-up.
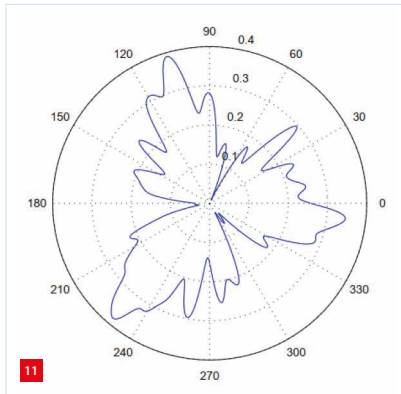
Repetitive radial run-out of the rotary stage (measured near the radial air-bearing plane).

Heat-pump compressor shaft for a two-stage compressor, with herringbone-grooved bearings and a 35-kW electric motor.

Optimal trade-off (blue dots) between rotor-dynamic stability (logarithmic decrement, corresponding to the natural log of the ratio of the amplitude of any two successive peaks of an excited oscillator) and system performance for a single-stage radial compressor for driving domestic-scale heat pumps. The system performance corresponds to the overall compressor efficiency (aerodynamic, mechanical and electrical losses) over a complete heating season. The star (yellow) highlights the solution obtained by individually optimising components.

computational power required to assess the performance metric response surface around the nominal design point.

To address this issue, Schiffmann's team has developed a framework to generate a set of neural-network-based 'surrogate' models (as opposed to purely analytical models) to enable the behaviour and performance prediction of rotors supported on herringbone-grooved journal bearings. Leveraging a non-dimensional representation of the rotor-dynamic equations of motion of the journal bearings, a universal model has been trained that predicts the whirl speed and the stability maps of typical rotors with a relative error of < 3% compared to experimentally validated high-fidelity models, while decreasing the computational burden by more than three orders of magnitude.

To benchmark the novel framework for robustness, two optimisations were performed. One where the rotor was optimised for maximum stability and minimum losses, and a second one where robustness was also considered as an objective for maximisation. For the first optimisation case, the robustness of the design was assessed after the optimisation.

The following bearing and rotor parameters have been taken into consideration:
• Clearance.
• Groove depth.
• Shaft dimensions.
• Position of herringbone-grooved journal bearings on the shaft.
• Gas properties.

The objectives and constraints set for the two optimisation cases are listed in Table 1.

Figure 14 shows the corresponding optimisation results. The coloured markers indicate the results of optimisation 2, which includes maximisation of design robustness, while the yellow star indicates the solution obtained by only maximising

Through this classical component-centred approach, the often very complex component interactions are neglected. Schiffmann aims for a holistic system approach and applies integrated design and optimisation methodologies to identify the ideal trade-off between competing design objectives such as rotor-dynamic performance and system efficiency.

In addition to actively working on integrated design and optimisation methodologies, Schiffmann's research team is also interested in identifying designs that, as well as maximising performance metrics, are also resilient in respect to manufacturing imperfection. This is particularly true for the design of gas-lubricated bearings, which require tight and accurate clearances. The challenge in identifying robust designs, i.e. maximising the feasible geometrical deviation around a nominal design, is the prohibitive increase in

Table 1
Optimisation cases 1 and 2.

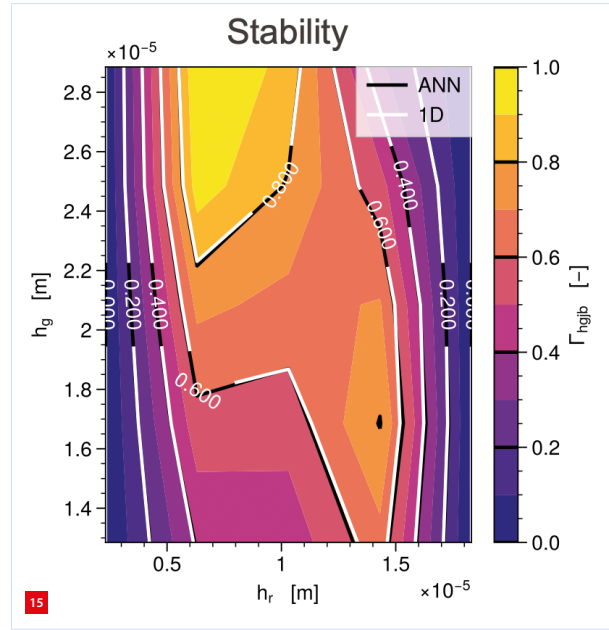|	Classical optimisation 1	Optimisation 2 for robustness
Objectives	• Maximum rotor-dynamic stability.	• Maximum hypervolume for deviations on bearing clearance and groove depth.
	• Minimum losses.	• Maximum signal-to-noise ratio across the feasible hypervolume.
		• Minimum losses.
Constraints	• Rotor-dynamic stability.	
	• Early lift-off (sufficient load capacity).	
	• Structural integrity.	
	• Lateral bending eigenmode sufficiently above the maximum rotor speed.	
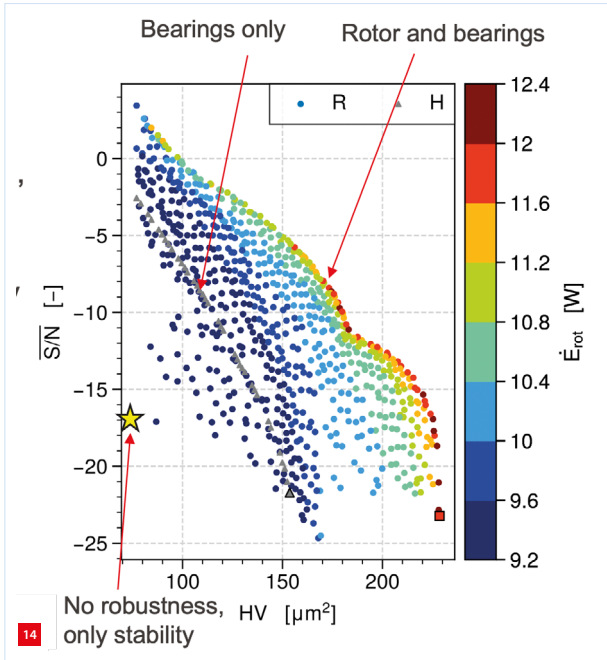
The Pareto Front (coloured markers), representing the set of efficient parameter ranges, obtained for maximising robustness (HV) and signal-to-noise ratio (S/N), and minimising the mechanical losses. The yellow star indicates the robustness performance obtained by only maximising rotor-dynamic performance and minimising losses. The highest HV/robustness is achieved with the square marker in the lower right region.

Logarithmic decrement of the rotor-dynamic stability as a function of the clearance (x-axis) and the groove depth (y-axis) for the most robust solution resulting from optimisation 2. The 1D white line represents the high-fidelity model, the dark line the artificial neural-network model.

stability and minimising losses. The results lead to the following conclusions. There is a trade-off between the three objectives of maximising the possible deviations in the bearing clearance and groove depth, and the signal-to-noise ratio (logarithm of the ratio between the average of the performance metric and its standard deviation across a sample of feasible solutions), and minimising the mechanical losses. Hence, a more robust solution (high HV) can be obtained by compromising on the signal-to-noise ratio and the losses.

HV or hypervolume corresponds to the n-dimensional volume spanned by the deviations of geometric variables around a nominal design point. In the case of two variables with deviations, such as clearance and groove depth, the HV corresponds to the area of the feasible deviations (i.e., tolerance bandwidth). Hence, in this case the HV corresponds to the feasible delta-clearance times and the feasible delta-groove depth.

An optimisation to maximise performance metrics such as the rotor-dynamic stability without considering robustness does not necessarily yield a robust solution. The hypervolume spanned by the solution from optimisation 1 is one order of magnitude smaller than the one obtained by optimisation 2.

The contour plot in Figure 15 highlights the logarithmic decrement of the rotor-dynamic stability (value above 0 for stable operation) as a function of the clearance (x-axis) and the groove depth (y-axis) for the most robust solution

resulting from optimisation 2. The plot suggests stable operation is possible with a radial clearance of 10 ± 8 mm and a groove depth of 21 ± 8 mm. For the solution from optimisation 1 without robustness (represented by the yellow star in Figure 14), the possible deviation on these features is ± 4 mm. The plot also compares the prediction using the high-fidelity model (white lines) with the ones from the neural-network-based surrogate model (black lines), suggesting an excellent agreement between the two models.

As well as the robustness optimisation, the loss and the load-carrying capacity can also be optimised with the help of similar graphs; they will tighten the tolerance bandwidth, but not to a large extent.
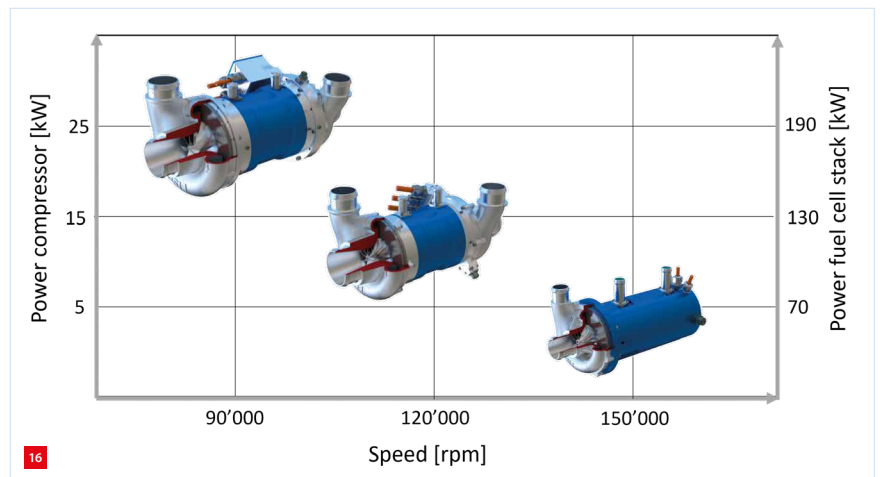
Compressor power and fuel-cell-stack power versus compressor speed for Fischer's compressor portfolio.

It appears that Schiffmann's work opens up a viable approach for obtaining robust shaft system designs with a reasonable amount of design simulation. Further work will also include aerodynamic turbomachinery design, thermal management and rotor layout. Also, the neural network will be the subject of a critical study and may be replaced or extended with physical models.

Non-dimensional analysis
Elia Iseli presented the small-scale turbomachinery technology of Fischer. The company develops compressors for hydrogen fuel cells in mobile applications for cars, ships and buses/trucks (Figure 16). Herringbone-grooved journal bearings are used, which provide the advantages of oil-free operation, avoidance of auxiliary systems, low frictional losses and a long lifetime.

Iseli highlighted the importance of investigating the following topics for developing robust compressor designs:
- Large eccentricities; influence of grooves.
- Rotor-dynamics.
- Reduction of computation time.
- Experimental validation.

For numerical analysis, methods were presented that involve linearised as well as transient approaches. The full transient method involves solving the transient, non-linear Reynolds equation on the grooved geometry domain. This is in contrast to the so-called Narrow Groove Theory (NGT), where an infinite number of grooves is assumed and the influence of the number of grooves is therefore not considered. As the transient solution of the Reynolds equation is very time consuming, a novel quasi-linear finite groove approach has been introduced, which is significantly faster while maintaining the possibility of considering a finite number of grooves. For large parameter variations, AI-based regression models of a two-layer feedforward neural network were introduced, which allowed for computing speed-up factors of up to 10^5.

For rotor-dynamic analysis, a rotor model with four degrees of freedom was used. The shaft properties consist of the mass m, the moments of inertia I_t and I_p (with t for transverse and p for polar), and the bearing positions with respect to the centre of gravity. The operational conditions are given by the gas properties (viscosity, pressure), the rotational speed and the forces acting on the rotor.

Iseli chose to describe the system with fully non-dimensional equations, which allows a systematic stability analysis without computing equal points multiple times (Figure 17).

Only the maximum non-dimensional mass and moment of inertia, defined by the hull curve, are relevant for guaranteeing stability. The hull curve can be defined for three regions. In region 1 the function is governed by the change of the rotational speed, in region 2 by the change of the ambient pressure, and in region 3 by the change of the viscosity. The hull curve helps the designer to limit the number of computations and facilitates the investigation of the solution space.

The following definitions apply:
- Non-dimensional mass for the three regions:

$$\hat{m}_{max} = \frac{mp_a}{36\mu^2 R}\frac{1}{(R/h_0)^5}\begin{cases}\Omega \in (0,\Omega_{max}), p_a = p_{a,max}, \mu = \mu_{min} \\ \Omega = \Omega_{max}, p_a \in (p_{a,max}, p_{a,min}), \mu = \mu_{min} \\ \Omega = \Omega_{max}, p_a = p_{a,min}, \mu \in (\mu_{min}, \mu_{max})\end{cases}$$

- Non-dimensional transverse moment of inertia:

$$\hat{I}_{t,max} = \hat{m}_{max}\frac{I_t}{mL_0^2}$$

- Compressibility number:

$$\Lambda = \frac{6\mu}{p_a}\left(\frac{R}{h_0}\right)^2\Omega\begin{cases}\Omega \in (0,\Omega_{max}), p_a = p_{a,max}, \mu = \mu_{min} \\ \Omega = \Omega_{max}, p_a \in (p_{a,max}, p_{a,min}), \mu = \mu_{min} \\ \Omega = \Omega_{max}, p_a = p_{a,min}, \mu \in (\mu_{min}, \mu_{max})\end{cases}$$

Here, m is the shaft mass, I_t the transverse moment of inertia, p_a the ambient pressure, μ the viscosity, R the radius of the bearing, h_0 the clearance, Ω the rotational speed, and L_0 the mid-plane distance between the two journal bearings.

Experimental validation with a representative test-rig set-up in terms of the rotating shaft/bearing set-up plus the dynamic measurement equipment showed that the numerical predictions were in good agreement with the experimental results.

Iseli concluded that the use of AI/neural networks in combination with non-dimensional analysis is key to reducing the simulation/calculation effort and provides the designer with useful tools for designing robust compressor systems by exploring large parameter spaces in a rapid way.
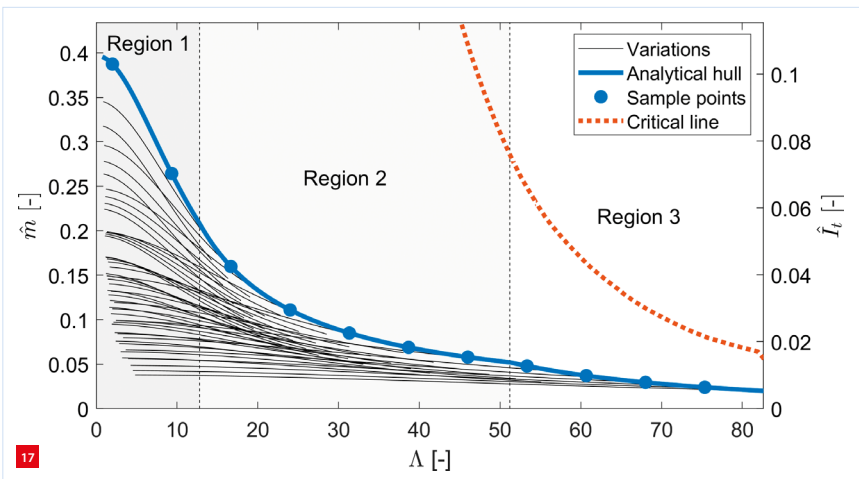
Non-dimensional mass and moment of inertia versus compressibility number. The hull curve encompasses all the dimensional variations. As long as the hull curve stays below the critical line, stability is guaranteed. (© EPFL, E. Iseli, "Numerical and experimental investigation of spiral-grooved gas journal bearings", thesis, 2022)